JPET Fast Forward. Published on October 8, 2003 as DOI:10.1124/jpet.103.056499

JPET #56499

Evidence for the involvement of a pulmonary first-pass effect via carboxylesterase in the disposition of a propranolol ester derivative after intravenous administration

Teruko Imai, Yasushi Yoshigae, Masakiyo Hosokawa, Kan Chiba, Masaki Otagiri

Faculty of Pharmaceutical Sciences, Kumamoto University, Kumamoto, Japan (T.I., Y.Y., M.O.) and Faculty of Pharmaceutical Sciences, Chiba University, Chiba, Japan (M.H., K.C.)

JPET #56499

A running title

Pulmonary first-pass effect via carboxylesterase

The corresponding author

Teruko Imai, Ph.D.

Faculty of Pharmaceutical Sciences, Kumamoto University, 5-1 Oe-honmachi, Kumamoto 862-0973, Japan

phone: +81-96-371-4626, fax: +81-96-371-4639

E-mail: iteruko@gpo.kumamoto-u.ac.jp

Number of text page:45

Number of tables: 4

Number of figures: 8

Number of references: 36

Number of words in the Abstract: 246

Number of words in the Introduction: 529

Number of words in the Discussion: 1493

ABBREVIATIONS

PL, propranolol; PNPA, *p*-nitrophenylacetate; BNPP, bis-nitrophenyl phosphate

A recommended section: Absorption, Distribution, Metabolism & Excretion

JPET Fast Forward. Published on October 8, 2003 as DOI: 10.1124/jpet.103.056499
This article has not been copyedited and formatted. The final version may differ from this version.

ABSTRACT

The disposition kinetics of *O*-butyryl propranolol (butyryl-PL), a model compound containing an ester moiety, after intravenous administration was compared with that of PL in rats and beagle dogs. Rats showed only 30% conversion of butyryl-PL to PL up to 2 hr after dosing, whereas dogs showed nearly complete conversion within 10 min after administration. The CL_{total} of butyryl-PL in rats was 5.8 L/hr/kg and that in dogs was 65.6±18.6 L/hr/kg, both of which were greater than hepatic blood flow. The *in vivo* conversion from butyryl-PL to PL in the rat could be explained on the basis of the hydrolysis characteristics in the liver and blood. The *in vitro* hydrolysis data and the *in vivo* data following intra-arterial administration clearly demonstrated that the extremely high CL_{total} of butyryl-PL in dogs was dependent on first-pass hydrolysis in the lung in addition to hydrolysis at a blood flow-limited rate in the liver and kidney. The availability of butyryl-PL after passage through the lung was 50%. Furthermore, the isoform of carboxylesterase involved in the pulmonary hydrolysis of butyryl-PL in the dog was identified as D1, a CES-1 group enzyme. However, butyryl-PL was not recognized as a substrate by CES-1 family carboxylesterases, which are present at high levels in the rat lung (RH-1) and kidney (RL-1). These findings indicate that extrahepatic metabolism,

especially in the lung, is important in the disposition of drugs containing an ester moiety after intravenous administration and that the substrate specificity of carboxylesterase isozyme distinguishes from others.

KEY WORDS

pulmonary first-pass effect, carboxylesterase, metabolism, *0*-butyryl-propranolol, enantioselective hydrolysis, plasma concentration

A number of ester- and amide-containing drugs have been clinically used in oral, cutaneous, and injectable formulations. The main route of detoxification or metabolic activation of these compounds is through enzymatic hydrolysis. Multiple carboxylesterases (E.C. 3.1.1.1) efficiently catalyze the hydrolysis of ester- and amide-containing drugs to their respective free acids, and these carboxylesterases are localized in the endoplasmic reticulum (ER) of a wide variety of organs and tissues in many mammalian species (Heymann, 1982; Satoh, 1987; Satoh and Hosokawa, 1998). In general, marked species differences are seen in esterase activity. For example, the level of esterase activity in mammalian liver microsomes is in the order dog>human>rat when *p*-nitrophenylacetate is used as the substrate, but is in the order dog>rat>human for isocarboxazid (Hosokawa et al., 1990). The different spectra of esterase activity for different substrates in various tissues lead to markedly divergent patterns of disposition after the administration of ester- and amide-containing drugs via various routes in mammalian species. Of all the animal tissues studied to date, the highest level of hydrolase activity is seen in the liver and a moderate level of hydrolase activity is seen in the proximal tubule of the kidney (Tsujita et al., 1988; Tsujita and Okuda, 1993). Interestingly, significant esterase activity has recently been found in the small intestine (Prueksaritanont et al., 1996; Yoshigae et al., 1998a), the skin

(McCracken et al., 1993; Ahmed et al., 1997), the heart (Dean et al., 1995), muscle (Nambu et al., 1987), the blood (Van Lith et al., 1992; McCracken et al., 1993; Ahmed et al., 1997), and the lung (McCracken et al., 1993; Dean et al., 1995; Forkert et al., 2001). Although hydrolase activity is observed in most tissues, ester- and amide-containing drugs are converted to free acid mainly by the hydrolase activity in the liver. Moreover, further metabolism in various organs complicates the disposition of drugs after administration to animals.

The present study focused on the extrahepatic metabolism by esterase, particularly pulmonary metabolism, as well as species differences in metabolism, using *O*-butyryl-propranolol (butyryl-PL; Fig.1), a PL ester derivative, as a model ester-containing compound. PL is distributed not only to the liver but also to several other tissues, including the lung, due to its hydrophobicity and basicity. Pang et al. (1982) has reported 50%-60% first-pass uptake of PL by the lung through a simple diffusion mechanism in dogs with cardiac catheterization. Dollery and Junod (1976) have reported the accumulation of PL in the rat lung. Butyryl-PL is more hydrophobic than PL and its basicity is comparable to that of PL ($\log P_{(\text{n-octanol/pH4.0 buffer})}$: PL, 0.38; butyryl-PL, 1.54; pKa: PL, 9.44; butyryl-PL, 9.02). Therefore, it is possible that butyryl-PL may be easily taken up and hydrolyzed to PL in the lung after intravenous administration.

In the present study, the disposition kinetics of butyryl-PL after intravenous administration was investigated in rats and beagle dogs. The tissues contributory to the hydrolysis of butyryl-PL were also identified in these two species. In addition, the extent of *in vivo* hydrolase activity in the lung was determined by comparison of intravenous and intra-arterial administration of butyryl-PL in beagle dogs. Furthermore, the isoform of carboxylesterase involved in pulmonary hydrolysis of butyryl-PL in the dog was identified.

JPET Fast Forward. Published on October 8, 2003 as DOI: 10.1124/jpet.103.056499
This article has not been copyedited and formatted. The final version may differ from this version.

MATERIALS AND METHODS

Materials

O-butyryl-PL hydrochloride was synthesized from PL hydrochloride (Wako Pure Chemical Industries, Ltd., Osaka, Japan) and butyryl chloride (Tokyo Kasei, Tokyo, Japan) according to the methods described previously (Shameem et al., 1993). The identity and purity of the synthesized butyryl-PL were confirmed by IR, NMR, atomic analysis, and HPLC. All other reagents used were of analytical grade.

Intravenous administration to rats and beagle dogs

Male Wistar rats (230–270 g, 8 weeks of age) and beagle dogs (9–11 kg, 1–3 years of age) were housed in an air-conditioned room with free access to commercial chow and tap water, and fasted for 15 hr prior to the intravenous administration of PL or butyryl-PL. PL (2.5 mg/400 μL/kg for rats, 2.0 mg/400 μL/kg for dogs) and equivalent doses of butyryl PL were dissolved in sterilized phosphate buffer (0.05M, pH 6.0). In rats, the solutions were injected via the femoral vein and blood samples were drawn from the jugular vein under ether anesthesia. In dogs, the solutions were injected via the right cephalic vein and

blood samples were drawn from the left cephalic vein without anethesia.

Intra-arterial administration of butyryl-PL to beagle dogs

Prior to intra-arterial administration to beagle dogs, a catheter (pig-tail angiocatheter, Goodman Co., Ltd. Nagoya, Japan) was advanced via the femoral artery until the tip was placed in the left ventricle. The dogs were anesthetized by the intra-muscular injection of atropine (0.005 mg/kg, Fuso Pharmaceutical Industry Ltd., Osaka, Japan), and further intra-muscular injection of mixture of ketamine hydrochloride (0.66 mg/kg, Sankyo Co., Ltd., Tokyo, Japan) and Xylazin hydrochloride (0.13 mg/kg, Bayer AG, Leverkusen, Germany). Proper placement of the catheter in the left ventricle was confirmed by monitoring the blood pressure. Four hours after arousal, butyryl-PL was injected into the left ventricle via the intra-arterial catheter. The butyryl-PL solution was the same as that used for i.v. injection (2 mg/400 μL/kg equivalent to PL). The catheter was flushed with phosphate-buffered saline solution (pH 6.0) to ensure that no butyryl-PL remained in the catheter before it was removed from the femoral artery.

Determination of plasma concentrations of PL and butyryl-PL

JPET Fast Forward. Published on October 8, 2003 as DOI: 10.1124/jpet.103.056499
This article has not been copyedited and formatted. The final version may differ from this version.

Blood samples (0.45 mL for rats, 1.0 mL for dogs) were drawn using heparinized syringes rinsed with a trace amount of paraoxon, an inhibitor of the hydrolysis of butyryl-PL. The plasma sample (200 µL) obtained from each blood sample after centrifugation (12,000*g* for 30 s) was added to 0.3 mL of 0.1M phosphate buffer (pH 4.0) saturated with NaCl. PL and butyryl-PL were then simultaneously extracted twice with 6 mL of ethyl acetate. Less than 1% of the butyryl-PL in the plasma degraded by following this procedure. The organic phase was evaporated to dryness and the residual material was redissolved in 50 µL of the mobile phase prior to the injection of a 20 µL aliquot into the HPLC system.

Data analysis for blood concentrations of PL and butyryl-PL

The blood level of each compound was calculated from the plasma concentration based on the blood/plasma ratio (Rb). The Rb was estimated from the drug concentrations in the plasma and blood after incubation of each compound in the blood, that was treated with 1 µM of paraoxon, for 10 min at 37°C. The mean Rb values of PL and butyryl-PL were constant over the concentration range from 10 to 1000 ng/mL. In addition, the Rb values of PL and butyryl-PL immediately after adding them in the blood were nearly same as those after 10min incubation. In rats, the Rb of (R)-PL and (S)-PL was 0.55 and 1.2, respectively, and that of

butyryl-PL was 0.88 for (R)-isomer and 0.91 for (S)-isomer. In dogs, the Rb of both (R)- and (S)-PL was 0.80, and that of butyryl-PL for both enantiomers was also 0.80. The racemic blood levels of PL and butyryl-PL were calculated as the sum of the blood concentrations of each enantiomer. The AUC from time zero to infinity ($AUC_{0-\infty}$) was calculated as the sum of the AUC of the mean blood concentration-time curve up to final sampling point by the trapezoidal rule and the AUC from the terminal exponential slope obtained by linear regression of the log-linear portion of the blood concentration profile. The apparent total body clearance was calculated as dose/$AUC_{0-\infty}$.

Organ clearance (CL_{org}) for liver and kidney was calculated by following equation; $CL_{org}=Q\cdot f_b\cdot CL_{int}/(Q+f_b\cdot CL_{int})$. Pulmonary clearance was calculated from $CL_{org}=f_b\cdot CL_{int}$. Intrinsic clearance ($CL_{int}$, L/hr/kg) was estimated from the Michealis-Menten kinetic parameters and protein content (mg/kg body) in respective organ according to the following equation; $CL_{int}=(V_{max}/K_m)$x(protein content), where protein content was 1280mg/kg for rat liver microsomes, 3218mg/kg for dog liver S9, 425mg/kg for dog lung S9, and 423mg/kg for dog kidney S9. The f_b (free fraction in blood) for butyryl-PL was calculated by f_p/Rb. The free fraction (f_p) of butyryl–PL in plasma treated with 1μM of paraoxon was determined by ultrafiltration method using a micropartition system MPS-1

JPET Fast Forward. Published on October 8, 2003 as DOI: 10.1124/jpet.103.056499
This article has not been copyedited and formatted. The final version may differ from this version.

(Amicon Co., Danvers, MA; a molecular weight cut off value of 30000). The f_p value of racemic butyryl-PL was 0.08 for rats and 0.07 for dogs. Then, f_b of butyryl-PL was calculated 0.09 for both dogs and rats. Q (tissue blood flow rate) listed in Table 1 was used for calculation.

A deconvolution method (Prueksaritanont et al., 1997) was used to calculate the systemic formation rate of PL after intravenous administration of butyryl-PL. Assuming that the disposition kinetics of PL and butyryl-PL was independent of each other and that their disposition kinetics were linear, the systemic formation rate (Rm) was calculated by following equation:

$$C_{Bu \rightarrow PL}(t) = \int_0^t Rm(\tau) \cdot C_{PL}(t - \tau)\, d\tau$$

where Rm is the systemic formation rate of PL from butyryl-PL, $C_{Bu \rightarrow PL}$ and C_{PL} are plasma PL concentration after intravenous administration of butyryl-PL and PL.

Preparation of microsomes and cytosol from various organs

Male beagle dogs (9–10 kg, 4–5 years of age) and male Wistar rats (230–270 g, 8 weeks of age) were used after overnight fasting with free access to water. The

dogs and rats were sacrificed by exsanguination under ether anesthesia. A cannula was place in the inferior vena cava, and the liver, kidneys and lungs were perfused with ice-cold 0.15M KCl to remove the blood. These organs were then resected, washed with ice-cold 0.15M KCl, and homogenized with 3 volumes of 10 mM phosphate buffer (pH 7.4) containing 0.15M KCl in a Potter-Elvehjem glass homogenizer equipped with a Teflon pestle under ice-cold conditions. The microsomes and cytosol fractions were prepared as described previously (Yoshigae et al., 1997). Briefly, the homogenate obtained (25% wet w/v) was centrifuged at 9,000*g* for 20 min at 4˚C to obtain the supernatant (S9) fraction. The S9 fraction was further centrifuged at 105,000*g* for 1 hr at 4˚C, and the resulting supernatant was used as the cytosolic fraction. The pellets were washed and resuspended by homogenization in phosphate buffer to obtain the microsomes solution. Protein content was determined by the method of Lowry et al. (1951) using bovine serum albumin as the standard protein, and the enzyme solutions were stored at -80˚C until use.

Hydrolysis experiments

Hydrolysis experiments were performed using subcellular fractions diluted with Tris-HCl buffer (50 mM, pH 7.4) according to the method described previously

(Yoshigae et al., 1997). The hydrolysis reaction was initiated by the addition of butyryl-PL after preincubation of each subcellular fraction for 5 min. The reaction was terminated by the addition of acetonitrile. In experiments involving inhibition by bis-*p*-nitrophenyl phosphate (BNPP), the enzyme solution was preincubated for 5 min with various concentrations of BNPP (final concentrations, 10^{-8} to 10^{-3} M) dissolved in dimethylsulfoxide (DMSO, 5 μL) or without esterase inhibitor (5 μL of DMSO alone) in controls. DMSO, a solvent for butyryl-PL and BNPP, was added to a final concentration of 1% v/v in the enzyme solution. The PL formed was determined by HPLC.

HPLC assay for enantiomers of PL and butyryl-PL

The HPLC assay was performed according to method described previously (Yoshigae et al., 1998b). The HPLC system comprised a Hitachi L-6000 pump with a loop-fitted Rheodine injector (volume: 20 μL), a Hitachi L-7480 fluorescence detector, and a Hitachi D-2500 chromato-integrator (Hitachi Co., Ltd., Tokyo, Japan). In the case of butyryl-PL, an ES-PhCD column (150×6.0 mm i.d., Shinwa Chemical Industries, Ltd., Kyoto, Japan) was used with a mobile phase of acetonitrile:20 mM KH_2PO_4 (45:55 v/v) at a flow rate of 0.8 mL/min. A Chiralcel OD column (25×0.46 cm i.d., Daisel Chemical Industries, Ltd., Tokyo,

Japan) was used for PL with a mobile phase of *n*-hexane:EtOH:diethylamine (85:15:0.6 v/v/v) at a flow rate of 0.6 mL/min. Both PL and butyryl-PL were detected with excitation and emission wavelengths of 285 and 340 nm, respectively.

Inhibition experiments for hydrolysis using anti-D1 polyclonal antibody

Anti-D1 polyclonal IgG was purified from anti-D1 rabbit serum using a Protein D column (Funakoshi, Tokyo, Japan) eluted with phosphate buffer (pH 3.0) containing 100 mM glycine. Microsomes from rat and dog tissues were incubated with anti-D1 IgG for 30 min at 37˚C in Tris-HCl buffer (pH 7.4). The mixtures were allowed to stand overnight at 4˚C and then centrifuged at 10,000*g* for 5 min. The resulting supernatant was used to assay hydrolase activity for butyryl-PL. The inhibition of activity by the antibody was calculated as the percentage of control activity using control rabbit IgG (Bayer AG, Leverkusen, Germany).

Polyacrylamide gel electrophoresis

Polyacrylamide gel electrophoresis (PAGE) was performed as described by Mentlein et al. (1980). Polyacrylamide gels (7.5% w/w) containing 1% w/v nonidet P-40 for solubilization of proteins were used for the separation of native

enzymes. After electrophoresis of the microsomal and cytosol samples (35-130 µg protein), the gels were stained for esterase activity with 1-naphtylbutyrate through coupling to liberated 1-naphthol with Fast Red TR-salt.

Immunochemical staining was carried out according to the method described previously (Hosokawa et al., 1987). Briefly, after SDS-PAGE was performed, the denaturing proteins were transferred from the acrylamide gels to a nitrocellulose membrane for 1 hr using an Atto semidry transfer unit. The membrane was blocked for 1 hr with 1.5% w/v bovine serum albumin solution in blocking buffer (0.1% w/v Tween 20, 25 mM Tris [pH7.4] and 150 mM NaCl). After the membrane was incubated with rabbit anti-D1 IgG for 1 hr, the membrane was rinsed three times with blocking buffer and was then incubated with goat antibody to rabbit IgG for 1 hr. After washing with blocking buffer, the membrane was processed using a Konica immuno-detection system for determining peroxidase activity (Konica Co., Ltd., Tokyo, Japan).

JPET Fast Forward. Published on October 8, 2003 as DOI: 10.1124/jpet.103.056499
This article has not been copyedited and formatted. The final version may differ from this version.

RESULTS

Blood concentrations of PL and butyryl-PL after intravenous administration

The plasma levels of PL and butyryl-PL after intravenous administration of PL and butyryl-PL to rats (2.5 mg/kg, equivalent to PL) and dogs (2.0 mg/kg, equivalent to PL) are shown in Fig. 2. After the intravenous administration of butyryl-PL to rats, the plasma concentrations of both intact butyryl-PL and converted PL were significantly lower than the plasma PL concentration from intravenously administered PL. In contrast, the temporal profile of PL converted from butyryl-PL after the intravenous administration of butyryl-PL in dogs was nearly the same as that of the intravenously administered PL, although the plasma concentration of intact butyryl-PL was markedly lower.

The apparent hydrolysis ratio from butyryl-PL to PL after intravenous administration was analyzed using the deconvolution method. The plasma levels of PL after the administration of butyryl-PL and after the administration of PL were used as the output and weight functions, respectively. The results of the analysis showed that only 30 % of the butyryl-PL was converted to PL up to 2 hr after administration in rats, whereas nearly complete conversion was observed within 10 min in beagle dogs (Fig. 3).

The AUC_{blood} and CL_{total} of PL and butyryl-PL after intravenous administration in

rats and dogs are listed in Table 1. In both species, the CL_{total} for PL was nearly the same as the hepatic blood flow due to high clearance via hepatic P450 metabolism, which in agreement with the findings of previous reports (George et al., 1976; Iwamoto and Watanabe, 1985). However, the CL_{total} of butyryl-PL in rats was about 1.5-fold greater than hepatic blood flow, and dogs showed a significantly increased CL_{total}, that was about 35-fold greater than hepatic blood flow and about 9-fold greater than cardiac output. In both species, particularly in the dog, the CL_{total} exceeded hepatic blood flow, indicating that extrahepatic metabolism contributed to the elimination of butyryl-PL.

In vitro hydrolysis in rat and dog tissues

In general, the liver is the most efficient organ for drug metabolism, but other organs such as the lung and kidney also often exhibit considerable drug metabolism activity. Moreover, high esterase activity is also present in the plasma. Therefore, the hydrolase activity for butyryl PL in these tissues was assayed to clarify the extrahepatic metabolism of butyryl-PL. As shown in Table2, the highest esterase activity for butyryl-PL in rats was observed in the liver microsomes, in contrast to significantly lower activities in the liver cytosol and in the lung and kidney preparations. The hydrolase activity of lung and kidney

microsomes was more than 60 times lower than that of liver microsomes. However, high levels of hydrolase activity for *p*-nitrophenylacetate (PNPA), a substrate for carboxylesterase, were observed in liver, kidney, and lung microsomes. These findings suggest that butyryl-PL is not easily recognized by the esterases in the rat lung and kidney.

On the other hand, dogs showed high hydrolase activity not only in the liver but also in the lung and the kidney, as shown in Table 2. The hydrolase activity in several organs (except for the plasma) was much higher in dogs than in rats. Although the order of hydrolase activity for butyryl-PL was liver>kidney≥lung, that for PNPA was liver≥lung>kidney. These findings suggest that substrate specificity varies in different tissues, possibly due to the expression of different esterases.

In addition, the hydrolase activity of rat plasma for butyryl-PL was 187±11.4 pmol/min/mg protein, which seemed quite low when compared to that of liver microsomes. This may have been due to a high protein content of plasma proteins such as albumin. In fact, the hydrolysis half-life of butyryl-PL (100 μM, 43.5 μg/mL) was about 4 min in rat plasma and 2.8 min in rat blood. In contrast, the hydrolase activity for butyryl-PL in dog plasma was 18.8±2.71 pmol/min/mg protein and its half-life was about 70 min. In addition, the hydrolysis half-life of

JPET Fast Forward. Published on October 8, 2003 as DOI: 10.1124/jpet.103.056499
This article has not been copyedited and formatted. The final version may differ from this version.

butyryl-PL in the blood was 31min, which was much shorter than that in plasma due to contribution of red blood cells to hydrolysis. However, the hydrolysis half-life of butyryl-PL in dog blood is markedly longer than the *in vivo* elimination half-life of butyryl-PL.

Estimation of organic clearance from *in vitro* hydrolysis parameters

The enzyme kinetic parameters, K_m and V_{max}, for hydrolase activity in tissue microsomes were estimated, and the organic clearance was then calculated from the K_m and V_{max} values based on a well-stirred model (Table3). The hepatic clearance of butyryl-PL in rat was nearly the same as the hepatic blood flow, indicating that butyryl-PL was hydrolyzed at a hepatic blood flow-limited rate in the rat liver. However, hepatic clearance accounted for only 60% of the CL_{total} after intravenous administration in the rat. The remaining 40% of the CL_{total} may have been due mainly to hydrolysis in the blood, showing a short half-life of 2.8 min, since hydrolase activity is quite low in the rat kidney and lung.

Organic clearance in dogs was estimated from the hydrolase activity in the S9 fraction due to the presence of hydrolase activity in both the micosome and cytosol fractions. The CL_{organ} of the liver was the same as the hepatic blood flow, indicating that butyryl-PL was hydrolyzed at hepatic blood flow-limited rate in

the dog liver. The CL_{organ} values of the lung and kidney were also high at 60% and 70% of the blood flow rate, respectively. Interestingly, the lung showed the highest CL_{organ} among these three organs. However, the *in vivo* CL_{total} (65.6 L/hr/kg) was much higher than the sum of the CL_{organ} values of these three organs (7.3 L/hr/kg). In general, an intravenously administered drug first enters the lung and is then distributed to the other organs via arterial blood flow. The above findings suggest that butyryl-PL is hydrolyzed by the first-pass effect through the lung before entering the systemic circulation in beagle dogs.

Intra-arterial administration of butyryl-PL to dogs

In order to demonstrate the extent of first-pass hydrolysis in the dog lung, butyryl-PL was administered intracardially as a route of administration that bypasses the lungs. Figure 4 shows that the plasma concentrations of PL converted from butyryl-PL after intra-arterial administration were significantly lower than those after intravenous administration. The AUCs of intact butyryl-PL after intra-arterial and intravenous administration of butyryl-PL were 67.1±28.7 ng·hr/mL and 30.5±8.6 ng·hr/mL, respectively, and their ratio (indicating availability of butyryl-PL after passage through the lung) was about 50%. These findings indicate that butyryl-PL undergoes first-pass hydrolysis in the lung in

beagle dogs.

Stereoselective hydrolysis and disposition of butyryl-PL

The R/S ratios of the hydrolase activities in various tissues in rats and dogs are listed in Table 2. Butyryl-PL was (R)-preferentially hydrolyzed in dog plasma, liver, lung, and kidney. In rats, the enantiospecificity of the hydrolysis of butyryl-PL differed in various tissues. In particular, (S)-preferential hydrolysis and non-enantioselective hydrolysis were observed in the liver and in the plasma, respectively.

Table 4 shows the AUC of each enantiomer of PL and butyryl-PL after the intravenous administration of racemic PL or racemic butyryl-PL to rats (2.5 mg/kg, equivalent to PL) and dogs (2.0 mg/kg, equivalent to PL). In rats, the AUC_{plasma} of (R)-PL after the intravenous administration of racemic PL was greater than that of its antipode, in agreement with the findings of previous reports (Vermeulen et al., 1992). However, the AUC_{blood} of PL was equivalent for the two enantiomers after correction based on the blood/plasma ratio (Rb: [R]-PL, 0.55±0.10; [S]-PL, 1.21±0.25). In addition, both the AUC_{plasma} and AUC_{blood} of (R)-butyryl-PL were 1.4-fold greater than those of the (S)-isomer after the intravenous administration of racemic butyryl-PL to rats. This may have been due to (S)-preferential hydrolysis of butyryl-PL in the rat liver. Moreover, the

AUC_{blood} of converted (R)-PL after the administration of butyryl-PL was higher than that of its antipode, possibly due to subsequent P450 metabolism of (S)-PL after (S)-preferential hydrolysis in the liver.

In dogs, the AUC_{plasma} and AUC_{blood} of PL after the intravenous administration of racemic PL were not significantly different for the two enantiomers. In addition, the AUC_{plasma} and AUC_{blood} of (S)-butyryl-PL were greater than those of (R)-butyryl-PL after the administration of racemic butyryl-PL in dogs, reflecting (R)-preferential hydrolysis in various tissues. However, the AUCs for the plasma and blood concentrations of PL converted from butyryl-PL were not enantioselective due to the nearly complete hydrolysis of both enantiomers within 10 min in various tissues, including the lung.

Inhibition of hydrolysis of butyryl-PL by BNPP

It has previously been demonstrated in inhibition experiments using several inhibitors for esterases that the hydrolysis of butyryl-PL in rat plasma and liver microsomes is catalyzed by carboxylesterase (Yoshigae et al., 1999). In order to identify the esterase involved in the hydrolysis of butyryl-PL in the dog liver and lung, BNPP was employed as a selective inhibitor of carboxylesterase. The relative activity against various BNPP concentrations (10nM–1mM) is shown in

Fig. 5. High concentrations of BNPP completely inhibited the hydrolysis of either enantiomer of butyryl-PL in microsomal fractions of the liver and lung, indicating that carboxylesterases are involved in the hydrolysis of butyryl-PL in these tissues. Moreover, BNPP inhibited the hydrolytic activity of cytosol in both tissues.

PAGE electrophoresis of subcellular fraction of the dog liver and lung

It is well known that the carboxylesterase activity present in microsomes is due to the binding of carboxylesterase to the ER (Satoh and Hosokawa. 1998). Despite the low hydrolase activity in the cytosol of any tissues in the rat, a relatively high cytosolic esterase activity was observed in the liver, lung and kidney in the dog. In order to distinguish cytosol esterases from microsomal esterases, nondenaturing gel electrophoresis was performed. As shown in Fig. 6, nondenaturing gel electrophoresis of liver microsomes revealed two electrophoretically distinct esterases with activity toward 1-naphtylacetate. Dog liver cytosol also showed two bands at the same positions as for microsomes, indicating the presence of esterases similar to those in microsomes. The kidney also showed two bands, whereas the lung showed only the upper band in both the cytosol and microsomal fractions. These findings indicate that the dog liver and kidney express two types of esterase but the lung expresses only one. Furthermore, it is suggested that the

cytosolic esterases are the same as the microsomal esterases in each tissue. Microsomal carboxylesterase that is loosely bound to the ER may leak into the cytosolic fraction during the preparation of homogenates.

Identification of carboxylesterase isozyme involved in the hydrolysis of butyry-PL

The microsomes from rat and dog tissues were subjected to SDS-PAGE and transferred electrophoretically to nitrocellulose for immunostaining. Anti-D1 polyclonal antibody, a specific antibody for dog liver carboxylesterase (D1), was used to detect the presence of the enzyme. In the results of immunostaining (Fig. 7), 60-kDa proteins were expressed in the lung and kidney but not in the small intestine in dogs. The cytosol showed an immunoblotting pattern similar to that of microsomes in dog tissues (data not shown), which supports the idea that carboxylesterase leaks from the microsomes during the preparation of homogenates. The 60-kDa protein was also expressed in the rat liver and lung but not in the rat small intestine. This protein might be a D1 cross-reactive carboxylesterase. Moreover, a protein of higher molecular weight was observed in the rat kidney.

The inhibition profiles of hydrolase activities for each enantiomer of butyryl PL by anti-D1 polyclonal antibody are shown in Fig. 8. The control rabbit IgG did

not have any influence on the hydrolase activity for butyryl-PL of the dog liver or lung microsomes, but specific anti-D1 polyclonal antibody inhibited 70% of the hydrolysis of both enantiomers of butyryl-PL in the liver and showed nearly complete inhibition in the lung. These findings indicate that D1 or cross-reactive carboxylesterases catalyze the hydrolysis of butyryl-PL in dog liver and lung. However, no inhibition by anti-D1-antibody was observed in the hydrolysis of butyryl-PL in rat liver microsomes.

Discussion

Carboxylesterases play an important role in the metabolism of endogenous compounds and exogenous substances such as drugs (including prodrugs), pesticides and herbicides. Carboxylesterases are widely distributed in the microsomes of the several tissues such as liver, kidney, brain and lung, where they are loosely bound to the luminal surface of the ER. The highest concentration of carboxylesterases is found in the liver microsomes (Morgan et al., 1994). Furthermore, it has been reported that secretory form such as serum carboxylesterase is highly expressed in rodent (Yan et al., 1995a). Therefore, the *in vivo* hydrolysis of drug containing ester moiety depends on hydrolase activity in the tissues as well as the blood.

Taking into account the drug disposition after administration, hydrophilic drugs are mainly distributed to the systemic blood circulation, while hydrophobic drugs distribute in several tissues. The hydrophobicity and basicity of butyryl-PL strongly suggest that butyryl-PL is distributed to several tissues, including the lung. Therefore, the blood concentrations of PL and butyryl-PL may be regulated by the hydrolytic activity in the respective tissues in each species. In fact, the markedly low blood levels of butyryl-PL observed after the intravenous administration of racemic butyryl-PL in dogs could not explain the hydrolysis in

the blood but the rapid hydrolysis of butyryl-PL in several tissues (Table 2).

It has been reported that PL is taken up into the lung by simple diffusion in the dog and that the lung has a capacity for 50%–60% first-pass uptake of PL (Pang et al., 1982). About 25% of administered PL accumulates in the isolated rat lung during a 5 min perfusion period through simple diffusion and a saturable pathway (Dollery and Junod, 1976). Therefore, butyryl-PL might also be taken up into the lung due to its higher hydrophobicity and similar basicity compared with PL. However, the intravenous administration of butyryl-PL resulted in marked differences in disposition in rats and dogs (Fig. 2). This divergence was mainly due to differences in pulmonary hydrolase activity in rats and dogs. In particular, dogs showed pulmonary first-pass hydrolysis in which about 50% of the administered butyryl-PL was hydrolyzed (Fig. 4). Furthermore, the hydrolysis of butyryl-PL in the liver and kidney at nearly same rate as tissue blood flow led to the rapid and complete conversion of butyryl-PL to PL in the dogs. However, rats showed the only 30% of conversion of butyryl-PL to PL up to 2 hr after intravenous administration, and the plasma concentrations of both butyryl-PL and PL were much lower than the plasma PL concentration when PL was administered to rats. These observations suggest that, in the rat, butyryl-PL is distributed to various tissues, including the lung, where esterase activity for butyryl-PL is low

(Table 2). After distribution to various tissues in the rat, butyryl-PL can remain in tissues with little hydrolase activity until it diffuse back into the blood and/or is detoxified to other metabolites. Furthermore, if butyryl-PL flows into the liver, which expresses esterase and P450, it may be sequentially metabolized to PL-metabolites after hydrolysis. The intrinsic clearance of PL for its P450 metabolism in the rat liver has been reported to be 810 L/hr/kg (Ishida et al., 1992) and 1690–2260 L/hr/kg (Gariépy et al., 1992) in *in vitro* experiments using rat liver microsomes and isolated perfused liver, respectively. Since these values are much larger than the intrinsic clearance by the hydrolysis of butyryl-PL in the rat liver (Table 3), PL is readily metabolized after the hydrolysis of butyryl-PL. The low PL concentration after the intravenous administration of butyryl-PL to the rat could be explained by retention in non-metabolizing tissues followed by sequential metabolism in the liver, which is the only major hydrolyzing tissue for butyryl-PL.

It has been demonstrated that the esterase responsible for pulmonary hydrolysis is D1 based on Western immunoblotting and the inhibition by anti-D1 antibody (Figs. 7 and 8). Carboxylesterase D1 is grouped in the CES-1 family according to the classification system proposed by Satoh and Hosokawa (1998). D1 is also expressed in the dog liver and kidney, and catalyzes the hydrolysis of butyryl-PL

to PL (Table 3). Western immunoblotting showed the presence of a cross-reacting enzyme against anti-D1 antibody in rat tissues. RH-1, RL-1, and hydrolase S, which are in the CES-1 family, are found in the rat lung. Particularly RH-1 is abundantly expressed in the lung (Gaustad et al., 1991; Yan et al., 1995b; Barr et al., 1998). On the other hand, the high levels of RL-1 in the kidney make it possible to evaluate its activity from the hydrolase activity in kidney microsomes. It has been reported that the molecular weight of RL-1 is 61 kDa, in contrast to 58 kDa for RH-1 (Hosokawa et al., 1987). In fact, the cross-reacting protein with anti-D1 antibody in the rat kidney showed a band at a higher molecular weight in Western immunoblotting (Fig. 7). Interestingly, butyryl-PL could not be hydrolyzed in the rat lung and kidney, indicating that RH-1 and RL-1 do not recognize butyryl-PL as a substrate despite their 78% and 66% homology with D1, respectively (Hosokawa et al., 2001). Actually, it has been reported that the hydrolysis of butyryl-PL in rat liver microsomes is not inhibited by anti-RH-1 antibody (Yoshigae et al., 1999). Hosokawa et al. (1990) have reported that RL-2 presents as a CES-1 isozyme in the rat liver and that RL-2 is characterized by its specific hydrolysis of 1-acyl glycerols (monoglycerides). A possible explanation for the hepatic hydrolysis of butyryl-PL might be the participation of RL-2.

In addition, rat esterase recognizes butyryl-PL as a specific substrate not only in

the liver but also in the small intestine (Yoshigae et al., 1998b). It is clear that CES-2 enzymes can catalyze the hydrolysis of butyryl-PL, because the CES-2 isozyme is highly express in the small intestine. The homology of CES-2 enzymes with CES-1 enzymes is less than 50%, and the isoelectric point of the CES-2 family (4.0–5.0) is lower than that of the CES-1 family (5.0–6.0). In general, both CES-1 and CES-2 enzymes are expressed in the liver of all mammalian species. The CES-2 enzyme also catalyzes the hydrolysis of butyryl-PL in rat liver microsomes. However, the major enzyme for hydrolysis of butyryl-PL is not CES-2 enzyme, because the enantioselectivity of the hydrolysis of butyryl-PL in the rat small intestine homogenate was opposite that observed in the liver (Yoshigae et al., 1998a). Further experiments are necessary to identify the CES isozyme responsible for the hydrolysis of butyryl-PL in the rat liver.

Similarly, the CES-2 isozyme is expressed in the dog liver and kidney. As shown in Fig. 6, the lower band in PAGE electrophoresis corresponds to the CES-2 enzyme. The finding that the hydrolase activity for butyryl-PL in the dog liver showed 70% inhibition by anti-D1 antibody despite complete inhibition by BNPP could be explained by the presence of D2, a dog CES-2 family carboxylesterase, contributory to the hydrolysis of butyryl-PL (Figs. 5 and 8). Moreover, D2 was also observed to contribute to the hydrolysis of butyryl-PL when the hydrolytic

activities for butyryl-PL and PNPA were compared in dog lung and kidney microsomes. The ratios of the hydrolysis of PNPA to that of butyryl-PL were 47 and 10 for lung microsomes and kidney microsomes, respectively (Table 2). Since the kidney, which contains both D1 and D2, was found to have a smaller value than the lung, which contains only D1, D2 might extensively catalyze the hydrolysis of buturyl-PL. With regard to the overlap in substrate specificity, it is interesting that butyryl-PL is not hydrolyzed by RH-1 and RL-1, which are grouped in the CES-1 family, despite the fact that CES-2 enzymes, which have less than 50% homology with the CES-1 family, also recognize butyryl-PL as a substrate.

The findings of the present study have demonstrated that pulmonary esterase activity is influenced by the disposition of drugs containing an ester-bond and that the species differences in pulmonary esterase activity are based on substrate specificities. A possible carboxylesterase that is present in the human lung is HU-1, a member of the CES-1 family, which has 78% homology with D1 (Munger ert al., 1991, Satoh and Hosokawa, 1998). It has been demonstrated that butyryl-PL is a good substrate for HU-1, which is found extensively in the human liver (Satoh and Hosokawa, 1998). These findings suggest the presence of first-pass metabolism of butyryl-PL in the human lung.

In addition to hydrolase activity in the liver and plasma, pulmonary metabolism is important in the elimination of drugs, but has rarely been studied due to problems inherent in the experimental methodologies currently available. Although *in vivo* methods have been applied to directly assess pulmonary first-pass metabolism in experimental animals, pulmonary metabolism can also be determined indirectly by conducting *in vitro* metabolic experiments employing lung homogenates. Moreover, commercially available human lung preparations are useful for evaluating pulmonary metabolism and for predicting the disposition of ester-containing drugs in human. Further kinetic studies concerning pulmonary metabolism are required in order to establish a suitable model for describing pulmonary metabolism *in vivo*.

REFERENCES

Ahmed S, Imai T, Yoshigae Y and Otagiri M (1997) Stereospecific activity and nature of metabolizing esterases for propranolol prodrug in hairless mouse skin liver and plasma. *Life Sci* **61**:1879–1887.

Barr F. Clark H and Hawgod S (1998) Identification of a putative surfactant convertase in rat lung as a secreted serine carboxylesterase. *Am J Physiol* **274**:L404–L410.

Dean RA, Zhang J, Brzezinski MR and Bosron WF (1995) Tissue distribution of cocaine methyl esterase and ethyltransferase activities: Correlation with carboxylesterase protein. *J Pharmacol Exp Ther* **275**:965-971.

Dollery CT and Junod AF (1976) Concentration of (+/–)–propranolol in isolated, perfused lungs of rat. *Br J Pharmacol* **57**:67-71.

Forkert P-G, Lee RP and Reis K (2001) Involvement of CYP2E1 and carboxylesterase enzymes in vinyl carbamate metabolism in human kung

microsomes. *Drug Metab Dispos* **29**:258–263.

Gariépy L, Fenyves D and Villeneuve J-P (1992) Propranolol disposition in the rat: variation in hepatic extraction with unbound drug fraction. *J Pharm Sci* **81**:255-258

Gaustad R, Sletten K, Lovhaug D and Fonnum F (1991) Purification and characterization of carboxylesterases from rat lung. *Biochem J* **274**:693–697.

George C F, Orme M L'E, Burabapong P, Macerlean D, Breckenridge A M and Dollery CT (1976) Contribution of the liver to overall elimination of propranolol. *J. Pharmacokin. Biopharm.* **4**: 17–27.

Heymann E (1982) Hydrolysis of carboxylic esters and amides. In *Metabolic Basis of Detoxification*, (Jakoby WB, Bend JR and Caldwell J eds) pp 229–245. Academic press, New York.

Hosokawa M, Maki T and Satoh T (1987) Multiplicity and regulation of hepatic microsomal carboxylesterases in rats. *Mol Pharmacol* 31:579–584.

Hosokawa M, Maki T and Satoh T (1990) Characterization of molecular species of liver microsomal carboxylesterases of several animal species and humans. *Arch Biochem Biophys* **277**: 219-227.

Hosokawa M, Suzuki K, Takahashi D, Mori M, Satoh T and Chiba K (2001) Purification, molecular cloning, and functional expression of dog liver microsomal acyl-CoA hydrolase: a member of the carboxylesterase multigene family. *Arch Biochem Biophys* **389**:245-253.

Ishida R, Suzuki K, Masubuchi Y, Narimatsu S, Fujita S and Suzuki T (1992) Enzymatic basis for the non-linearity of hepatic elimination of propranolol in the isolated perfused rat liver. *Biochem Pharmacol* **44**:2281–2288.

Iwamoto K and Watanabe J (1985) Dose-dependent presystemic elimination of propranolol due to hepatic first-pass metabolism in rats. *J Pharm Pharmacol* **37**:826-828

Lowry OH, Rosebrough NJ, Farr AL and Randall RJ (1951) Protein measurement

with the folin phenol reagent. *J Biol Chem* **193**: 264–275.

McCracken NW, Blain PG and Williams FM (1993) Nature and role of xenobiotic metabolizing esterases in rat liver, lung, skin and blood. *Biochem Pharmacol* **45**:31-36.

Mentlein R, Heiland S and Hwymann E (1980) Simultaneous purification and comparative characterization of six serine hydrolases from rat liver microsomes. *Arch Biochem Biophys* **200**:547–559.

Morgan EW, Yan B, Greenway D, Petersen DR and Parkinson A (1994) Purification and characterization of two rat liver microsomal carboxylesterase (hydrolase A and B). *Arc Biochem Biophys* **315**:495-512.

Munger JS, Shi GP, Mark EA, Chin DT, Gerard C and Chapman HA (1991) A serine esterase released by human alveolar macrophages is closely related to liver microsomal carboxylesterase. *J Biol Chem* **266**:18832–18838.

Nambu K, Miyazaki H, Nakanishi Y, Oh-e Y and Matsunaga Y (1987) Enzymatic hydrolysis of haloperidol decanoate and its inhibition by proteins. *Biochem*

Pharmacol **36**:1715–1722.

Pang JA, Blackburn JP, Butland RJ, Corrin B, Williams TR and Geddes DM (1982) Propranolol uptake by dog lung: Effect of pulmonary artery occlusion and shock lung. *J Appl Physiol Respiratory Environm Exer Physiol* **52**:393–401.

Prueksaritanont T, Gorham LM, Hochman JH Tran LO and Vyas KP (1996) Comparative studies of drug-metabolizing enzymes in dog, monkey, and human small intestines, and Caco-2 cells. *Drug Metab Dispos* **24**:634–642 .

Prueksaritanont T, Gorham LM, Yeh KC (1997) Analysis of metabolite kinetics by deconvolution and in vivo-in vitro correlations of metabolite formation rates: studies of fibrinogen receptor antagonist ester prodrugs. *J Pharm Sci* **86**:1345-1351.

Satoh T (1987) Role of carboxylesterases in xenobiotic metabolism. In *Reviews in Biochemical Toxicology*. (Benda JR, Hodgston BE and Philpot RM eds) 155–181, Elsevier, New York.

Satoh T and Hosokawa M (1998) The mammalian carboxylesterases: From

molecule to functions. *Ann Rev Pharmacol Toxicol* **38**:257–288.

Shameem M, Imai T and Otagiri M (1993) An in-vitro and in-vivo correlative approach to the evaluation of ester prodrugs to improve oral delivery of propranolol. *J Pharm Pharmacol* **45**:246-252.

Tsujita T, Miyata T and Okuda H (1988) Purification of rat kidney carboxylesterase and its comparison with other tissue esterases. *J Biochem* **103**:327–331.

Tsujita T and Okuda H (1993) Palmitoyl-coenzyme A hydrolyzing activity in rat kidney and its relationship to carboxylesterase. *J Lipid Res* **34**:1773–1781.

Van Lith HA, Haller M, Van Zutphen LF and Beynen AC (1992) The use of three ferguson-plot-based calculation methods to determine the molecular mass of proteins as illustrated by molecular mass assessment of rat-plasma carboxylesterase ES-1, ES-2 and ES-14. *Anal Biochem* **201**:288–300.

Vermeulen M, Belpaire F M, Moerman E, Smet F and Bogaert M G (1992) The

influence of aging on the stereoselective pharmacokinetics of propranolol in the rat. *Chirality* **4**:473–479.

Yan B, Yang D, Bullock P and Parkinson A (1995a) Rat serum carboxylesterase; cloning, expression, regulation and evidence of secretion from liver. *J Biol Chem* **270**:19128–19134.

Yan B, Yang D, Brady M and Parkinson A (1995b) Rat testicular carboxylesterase: Cloning, cellular localization, and relationship to liver hydrolase A. *Arc Biochem Biophys* **316**:899–908.

Yoshigae Y, Imai T, Horita A, Otagiri M (1997) Species differences for stereoselective hydrolysis of propranolol prodrugs in plasma and liver. *Chilarily* **9**:661–666

Yoshigae Y, Imai T, Horita A, Matsukane H and Otagiri M (1998a) Species differences in stereoselective hydrolase activity in intestinal mucosa. *Pharm Res* **15**:626–631.

Yoshigae Y, Imai T, Aso T, Otagiri M (1998b) Species differences in the disposition of propranolol prodrugs derived from hydrolase activity in intestinal mucosa. *Life Sci* **62**:1231–1241.

Yoshigae Y, Imai T, Taketani M and Otagiri M (1999) Characterization of esterases involved in the stereoselective hydrolysis of ester-type prodrugs of propranolol in rat liver and plasma. *Chirality* **11**:10–13.

JPET Fast Forward. Published on October 8, 2003 as DOI: 10.1124/jpet.103.056499
This article has not been copyedited and formatted. The final version may differ from this version.

Figure Captions

Figure 1

Structure of butyryl-PL

Figure 2

Plasma concentrations of PL and butyryl-PL after intravenous administration of PL and butyryl-PL in rats and dogs (2.5 mg/kg for rats and 2.0 mg/kg for dogs, equivalent to PL).

Symbols indicate PL administration (···▲··), butyryl-PL (●) and PL (○) after butyryl-PL administration. Values are mean±s.d. (n=4).

Figure 3

Apparent hydrolysis ratio of butyryl-PL after intravenous administration to rats (●) and dogs (○).

The hydrolysis ratio was calculated by the deconvolution method.

The plasma PL concentration profiles after intravenous administration of butyryl-PL and PL were used as the output function and weight function, respectively.

Figure 4

Plasma concentrations of PL and butyryl-PL after intra-arterial and intravenous administration of butyryl-PL (2.0 mg/kg, equivalent to PL) in dogs.

The circles and triangles indicate intravenous and intra-arterial administration, respectively. Open and closed symbols indicate the concentrations of converted PL and intact butyryl-PL, respectively. *: $p<0.05$ compared with intra-arterial administration. Values are mean±s.d. (n=4).

Figure 5

Inhibition of the hydrolysis of each butyryl-PL enantiomer in dog liver and lung microsomes by BNPP.

BNPP concentrations were 10nM–1mM. Remaining activity values (○: [R]-isomer, ●: [S]-isomer) were plotted against the logarithm of mol of BNPP per g protein of microsomes. Values are mean±s.d. (n=3).

Figure 6

Nondenaturing gel electrophoresis of dog tissue microsomes and cytosol.

Staining for esterase activity was based on the formation of a red insoluble

complex between Fast Red TR and 1-naphtol, which was released enzymatically from 1-naphthylacetate. Lanes 1-6 contained 35µg protein except Lane 4 (130µg protein). Lane 1: lung cytosol, Lane 2: lung microsomes, Lane3: kidney microsomes, Lane 4: kidney cytosol, Lane 5: liver microsomes, Lane 6: liver cytosol.

Figure 7

Immunoblots of microsomes from various tissues of the rat and dog probed with anti-D1 IgG.

Microsomes from rat and dog tissues were subjected to SDS-PAGE and transferred electrophoretically to nitrocellulose for immunostaining. Lanes 1-8 contained 5 µg protein. Lane 1: dog liver, Lane 2: dog lung, Lane 3: dog kidney, Lane 4: dog small intestine, Lane 5: rat liver, Lane 6: rat lung, Lane 7: rat kidney, Lane 8: rat small intestine.

Figure 8

Effects of polyclonal anti-D1 antibodies on the hydrolase activities for each butyryl PL enantiomer in dog liver and lung microsomes and in rat liver microsomes.

Remaining activity values (open symbols: [R]-isomer, closed symbols: [S]-isomer) were plotted against the ratio of protein contents of IgG and microsomes. Circles and triangles indicate the presence of rabbit IgG (control) and anti-D1 IgG, respectively. Values are the mean ± s.d. (n=3). *: $p<0.05$ compared with rabbit IgG (control).

JPET Fast Forward. Published on October 8, 2003 as DOI: 10.1124/jpet.103.056499
This article has not been copyedited and formatted. The final version may differ from this version.

Table 1. AUC_{blood} and total clearance (CL_{total}) of PL and butyryl-PL after intravenous administration in rats and dogs

Dosing compound		Rat*	Dog
PL	$AUC_{blood,PL}$	649	1052±219
	$CL_{total,PL}$	3.85	1.90±0.61
Butyryl-PL	$AUC_{blood,Bu}$	433	30.5±8.60
	$AUC_{blood,Bu\rightarrow PL}$	289	1103±310
	$CL_{total,Bu}$	5.77	65.6±18.6
Blood flow	Liver	3.6	1.9
	Cardiac output	17.8	7.2

AUC:ng·hr/mL, CL and blood flow: L/hr/kg.

*Parameters were calculated from mean blood concentration after intravenous administration of PL and butyryl-PL in rats (2.5 mg/kg for rats, equivalent to PL). AUC of drugs after administration in rats was calculated from mean plasma concentrations from time zero to infinity. $AUC_{blood} = AUC_{plasma} \times Rb$. $AUC_{blood,PL}$ means the AUC_{blood} of PL after administration of PL. $AUC_{blood,\ Bu}$ and $AUC_{blood,\ Bu\rightarrow PL}$ mean the AUC_{blood} of butyryl-PL and PL after administration of butyryl-PL, respectively.

$CL_{total,PL}$ and $CL_{total,Bu}$ mean the total clearance of PL and butyryl-PL after administration of PL and butyryl-PL, respectively.

Table 2. Hydrolysis activity of plasma, liver, kidney, and small intestinal mucosa

	Rat			Dog		
Tissue	Total activity for R- and S-butyryl-PL	R/S ratio	Activity for PNPA butyryl-PL	Total activity for R- and S-butyryl-PL	R/S ratio	Activity for PNPA
Plasma (pmol/min/mg protein)						
	187±11.4	1.13		18.8±2.71	5.36	
Liver (nmol/min/mg protein)						
Microsomes	172±25.4	0.39	3550±733	363±35.5	2.59	6750±276
Cytosol	1.47±0.26	0.49	109±19.87	3.78		
Lung (nmol/min/mg protein)						
Microsomes	1.93±0.08	2.39	350±35.7	131±7.37	3.08	6130±357
Cytosol	1.64±0.17	1.59		43.3±5.30	3.04	
Kidney (nmol/min/mg protein)						
Microsomes	2.78±0.19	0.40	928±138	183±10.8	2.80	1820±48.9
Cytosol	1.36±0.09	0.87		16.2±0.59	1.94	

JPET Fast Forward. Published on October 8, 2003 as DOI: 10.1124/jpet.103.056499
This article has not been copyedited and formatted. The final version may differ from this version.

Table 3 Enzyme kinetic parameters of rat liver microsomes and dog liver, lung, and kidney 9000*g* supernatants for butyryl-PL and its organ clearance (CL_{org}) estimated from *in vitro* data

Tissue	K_m	V_{max}	CL_{int}	CL_{org}	Blood flow (Q)
	(μM)	(nmol/min/mg protein)	(L/hr/kg)	(L/hr/kg)	(L/hr/kg)
Rat					
Liver	180±21.8	709±19.3	304±27.5	3.3	3.6
Dog					
Liver	62.5±0.60	292±10.0	901±37.3	1.9	1.9
Lung	65.3±10.4	120±14.4	50.1±7.01	4.5	7.2
Kidney	132±22.6	180±30.7	34.7±4.10	0.9	1.3

Protein content of rat liver microsomes is 1280mg/kg. Protein content of S9 fraction of dog liver, lung, and kidney is 3220mg/kg, 425mg/kg, and 423mg/kg, respectively. Unbound fraction of butyryl-PL in blood (f_b) was 0.09. CL_{int} was calculated by $V_{max}/K_m\times$ (protein content). CL_{org} for liver and kidney was calculated by $Q\times f_b\times CL_{int}/(Q+f_b\times CL_{int})$, and that for lung was calculated by $f_b\times CL_{int}$.

JPET Fast Forward. Published on October 8, 2003 as DOI: 10.1124/jpet.103.056499
This article has not been copyedited and formatted. The final version may differ from this version.

Table 4. AUC (ng·hr/mL) and CL_{total} (L/hr/kg) of each enantiomer after intravenous administration of racemic PL and butyryl-PL to Rats (2.5 mg/kg, equivalent to PL) and dogs (2.0 mg/kg, equivalent to PL)

	Rat			Dog		
Administration	R-isomer	S-isomer	R/S ratio	R-isomer	S-isomer	R/S ratio
PL						
$AUC_{plasma, PL}$	610	255	2.4	648±231	672±221	0.96±0.08
$AUC_{blood, PL}$	336	309	1.1	517±170	539±177	0.96±0.07
$CL_{total,PL}$	3.71	4.02	0.92	1.93±0.61	1.85±0.60	0.98±0.09
Butyryl-PL						
$AUC_{plasma, Bu}$	281	199	1.4	7.51±3.81	25.1±3.89	0.30±0.06
$AUC_{blood, Bu}$	250	180	1.4	6.12±3.09	20.1±3.11	0.30±0.06
$AUC_{plasma, Bu\rightarrow PL}$	272	89.1	3.1	621±185	634±222	0.98±0.05
$AUC_{blood, Bu\rightarrow PL}$	150	108	1.4	496±147	508±178	0.98±0.06
$CL_{total,Bu}$	5.01	6.90	0.73	165±84.4	49.8±7.71	3.3±1.1

AUC of drugs after administration in rats was calculated from mean plasma concentrations from time zero to infinity. Rb values in the rat: (R)-PL, 0.55; (S)-PL, 1.2; (R)-butyryl-PL, 0.88; (S)-butyryl-PL, 0.91. Rb values in the dog: (R)-PL, 0.80; (S)-PL, 0.80; (R)-butyryl-PL, 0.81; (S)-butyryl-PL, 0.80. AUC_{blood} was calculated by AUC_{plasma} multiplied by Rb. CL_{total} was calculated from Dose/AUC_{blood}.

JPET Fast Forward. Published on October 8, 2003 as DOI: 10.1124/jpet.103.056499
This article has not been copyedited and formatted. The final version may differ from this version.

Figure 1

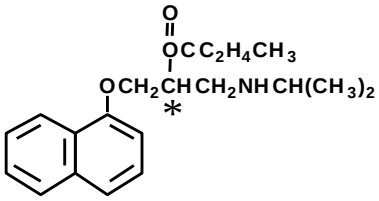

***O*-Butyryl Propranolol**
(Butyryl-PL)

JPET Fast Forward. Published on October 8, 2003 as DOI: 10.1124/jpet.103.056499
This article has not been copyedited and formatted. The final version may differ from this version.

Figure 2

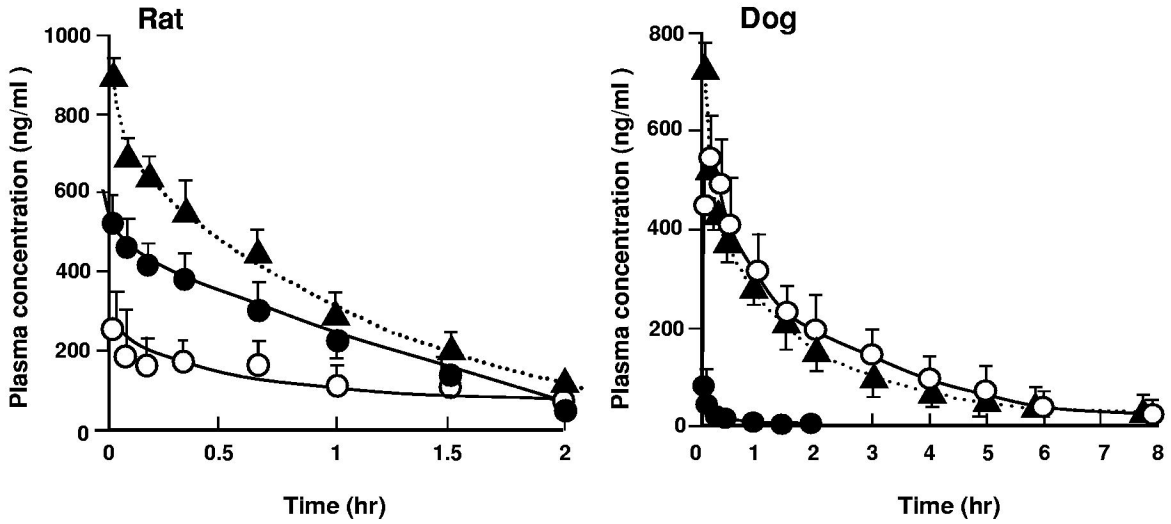

JPET Fast Forward. Published on October 8, 2003 as DOI: 10.1124/jpet.103.056499

Figure 3

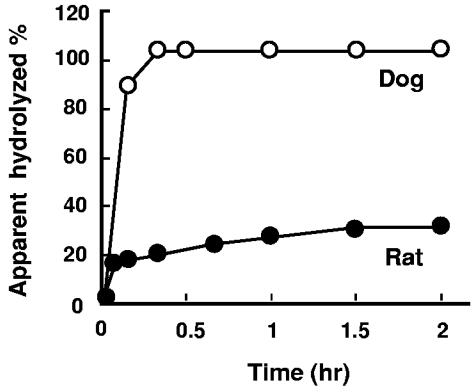

JPET Fast Forward. Published on October 8, 2003 as DOI: 10.1124/jpet.103.056499
This article has not been copyedited and formatted. The final version may differ from this version.

Figure 4

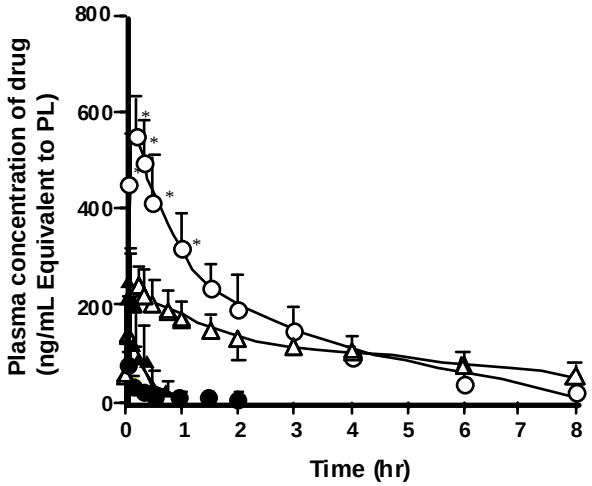

JPET Fast Forward. Published on October 8, 2003 as DOI: 10.1124/jpet.103.056499

Figure 5

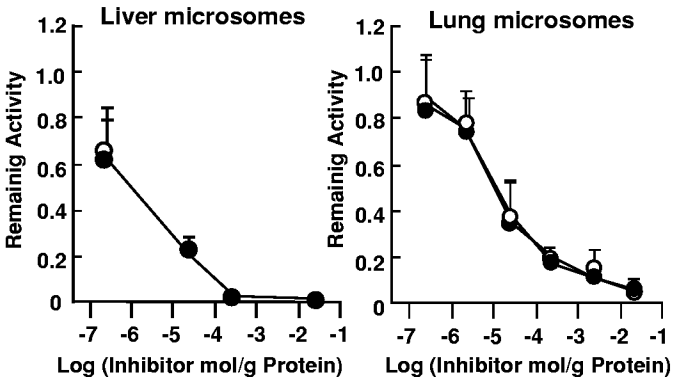

JPET Fast Forward. Published on October 8, 2003 as DOI: 10.1124/jpet.103.056499
This article has not been copyedited and formatted. The final version may differ from this version.

Figure 6

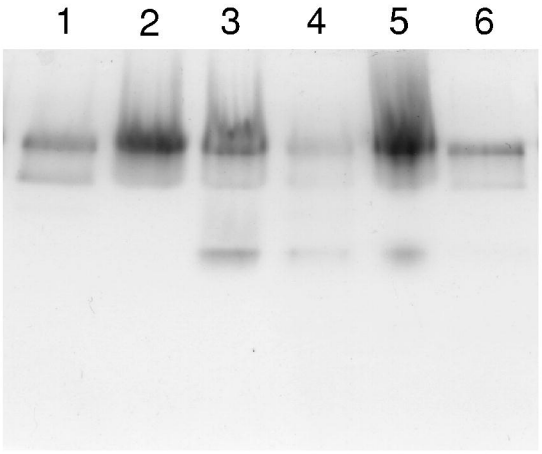

JPET Fast Forward. Published on October 8, 2003 as DOI: 10.1124/jpet.103.056499

Figure 7

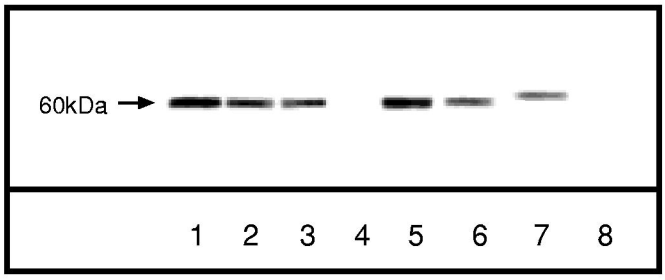

JPET Fast Forward. Published on October 8, 2003 as DOI: 10.1124/jpet.103.056499
This article has not been copyedited and formatted. The final version may differ from this version.

Figure 8